Supporting Information

Photothermal Stimuli-Responsive Biocomposites Based on Cross-linked Poly($_L$-malic acid) Reinforced with Carbon Nanotubes

Qianru Wanyan[1] Yaxin Qiu[1] Juqun Xi[2] Suna Yin[1] Wenting Zhang[1] Defeng Wu[1,3*]

([1] School of Chemistry & Chemical Engineering, Yangzhou University, Yangzhou, Jiangsu Province, 225002, P. R. China)

([2] Medical College, Yangzhou University, Jiangsu, 225002, P. R. China)

([3] Provincial Key Laboratories of Environmental Engineering & Materials, Yangzhou, Jiangsu Province, 225002, P. R. China)

[*] Corresponding author. Tel.: +86 514 87975230; Fax: +86 514 87975244; E-mail address: dfwu@yzu.edu.cn.

Video S1. Shape-memory behavior of S-shaped nanocomposite sample with 0.3 wt% CNTs under the 90 ^{o}C thermal environment.

Video S2. Fixing process of temporary shape (S-shape) of the nanocomposite ribbon with 0.3 wt% CNTs (deformed at 80 ^{o}C and fixed in the 20 ^{o}C air) (2X).

Video S3. Shape-memory behavior of S-shaped nanocomposite sample with 0.3 wt% CNTs trigged by near infrared light (650 nm, 50 mW cm^{-2}) (8X).

Table S1. Thermal and mechanical parameters of PLMA/CNT nanocomposites with various CNT loadings

samples	T_g (°C)	tensile strength (MPa)	Young's modulus [a] (GPa)	Young's modulus [b] (GPa)	elongation (%)
PLMA	73.8	60.02±2.03	1.46±0.15	1.97	5.3
0.1 wt%	79.5	62.82±1.06	1.50±0.20	2.07	6.8
0.2 wt%	86.8	67.65±8.28	2.08±0.20	2.26	5.5
0.3 wt%	87.3	79.80±5.27	1.83±0.25	2.39	7.8
0.4 wt%	85.8	69.80±6.96	1.84±0.18	2.38	7.9
0.5 wt%	85.6	65.90±3.82	1.79±0.15	2.42	6.8
0.8 wt%	81.8	65.67±3.91	1.82±0.20	2.18	7.3
1.0 wt%	82.3	61.25±0.43	1.80±0.12	1.95	8.3
0.2 wt% [c]	75.3	63.80±3.86	1.68±0.25	-	4.6

a: obtained from tensile tests; *b*: from DMA tests; *c*: prepared by physical mixing.

Table S2. Thermal and structural parameters of shape memory performance of PLMA and its nanocomposites

samples	fixing temp. (T_f) °C	recovery temp. (T_r) °C	shape fixity ratio (R_f) %	shape recovery ratio (R_r) %
PLMA	30	90	93.73	99.98
0.1 wt%	30	90	92.69	99.25
0.3 wt%	30	90	94.79	99.53
0.5 wt%	30	90	96.57	99.99
0.8 wt%	30	90	93.39	99.98

Notes: the shape fixity ratio (R_f) and shape recovery ratio (R_r) are calculated according to:

$$R_f = \frac{\varepsilon_{S1} - \varepsilon_{S0}}{\varepsilon_{S0,\,load} - \varepsilon_{S0}}, \quad R_r = \frac{\varepsilon_{S0,\,recover} - \varepsilon_{S0}}{\varepsilon_{S1} - \varepsilon_{S0}} \qquad (1)$$

where ε_{S0} is the primary strain, $\varepsilon_{S0,\,load}$ is the strain under load, ε_{S1} is temporary shape in the strain without load, and $\varepsilon_{S0,\,recover}$ the strain after recovery. The nanocomposite samples possess T_g ranged in 79-87 °C (**Table S1**), which highly depend on the degree of crosslinking and dispersion of CNTs. The samples with 0.2-0.3 wt% CNTs have the highest T_gs because of synergistic effects of their good CNT dispersion and higher degrees of bulk crosslinking (**Figure 2**). The recovery temperature was determined as 90 °C, and at this temperature, all samples present very good R_r, with the values almost to 100%, and their R_rs range in 93-96%, with no evident difference. This means that the shape memory behavior of the nanocomposites, especially their shape recovery is not highly dependent on the bulk properties such as moduli and degrees of crosslinking of PLMA within the experimental CNT loading ranges (0.1-1.0 wt%) at testing temperature 90 °C.

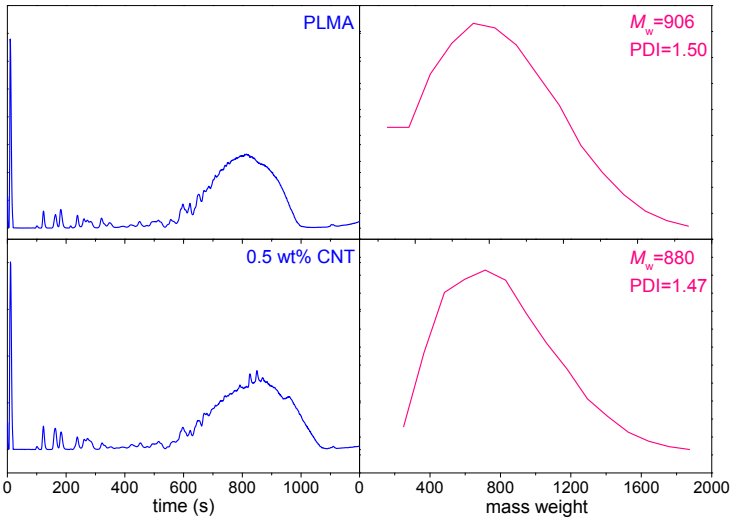

Figure S1. HPLC-MS spectra of PLMA prepared by polycondensation with and without CNTs (left) and corresponding integrated curves calculated by the intensities of the fractions with various molecular weights (right)

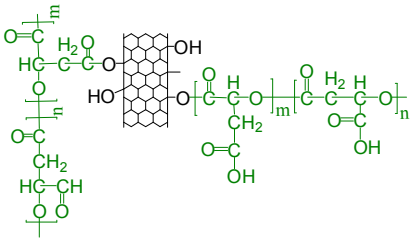

Figure S2. Schematics of graft reactions of CNTs

Note: The monomer *l*-malic acid could react with hydroxyl groups of CNTs, forming grafted PLMA chains during polycondensation.

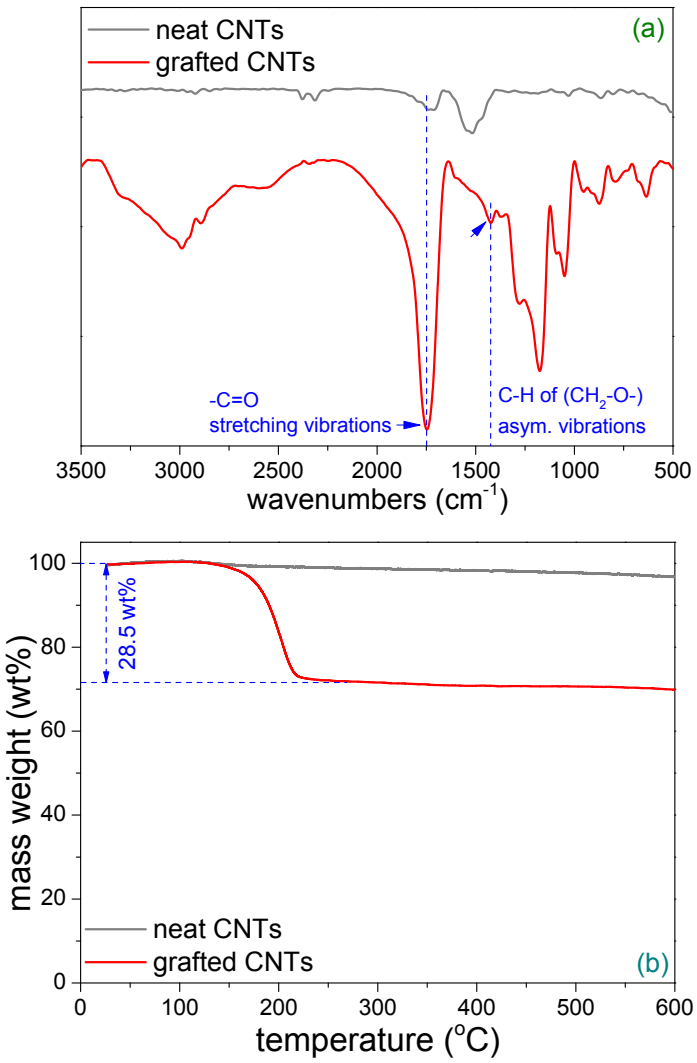

Figure S3. (a) FT-IR spectra and (b) TGA curves of blank CNTs and extracted ones after grafting reaction

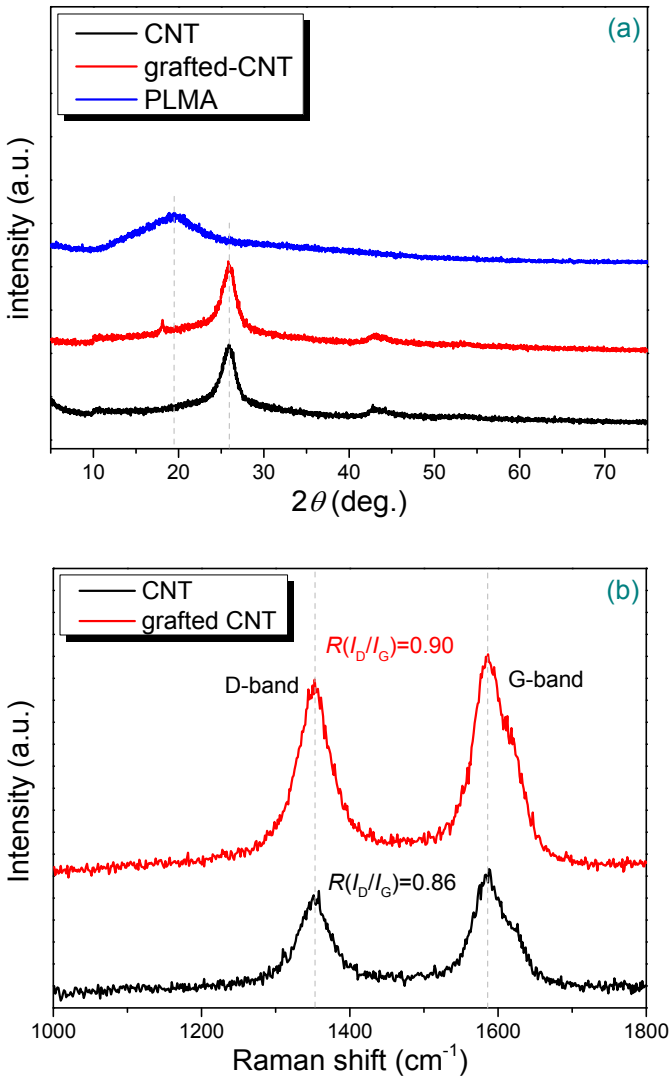

Figure S4. (a) XRD and (b) Raman spectra of blank CNTs and extracted ones after grafting reaction

Note: XRD spectra shown in (a) reveal that grafting reaction did not break the surface structure of CNTs down, whereas leading to the formation of defects, which is confirmed by increased I_D/I_G ratio shown in Raman spectra (b).

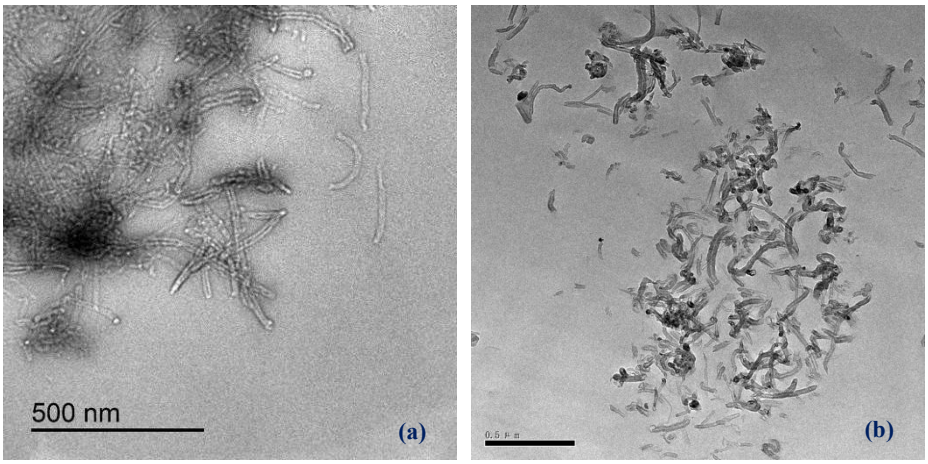

Figure S5. TEM image of (a) the nanocomposite with 0.2 wt% CNTs prepared by the way of physical blending and (b) the nanocomposite with 0.5 wt% CNTs prepared by via *in-situ* crosslinking

Note: In the composite sample prepared via the physical blending (the pristine CNTs were added into reactive system in the crosslinking stage, instead of during polycondensation of *L*-malic acid, which means that there were no grafted PLMA chain on the surfaces of CNTs), CNTs were mainly dispersed as highly self-entangled aggregates, showing very poor dispersion and distribution in the cross-linked matrix.

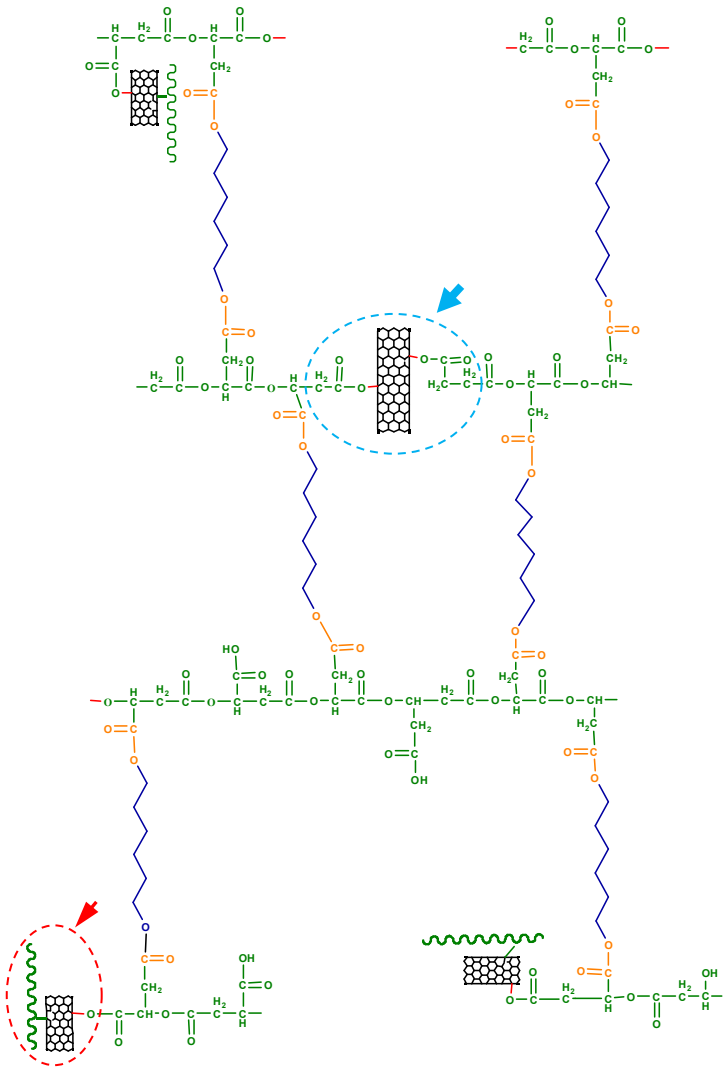

Figure S6. Schematics of crosslinking networks of PLMA/CNT nanocomposites

Note: The grafted CNTs could act as the crosslinking points (see blue arrow), participating in the formation of effective crosslinking network structure; or as the ineffective points (see red arrow), linked with the networks through esterification, forming pendulous particles-like structure. Some CNTs could be dispersed as inert particles, distributed well in the PLMA matrix because improved polymer-CNT affinity resulted from surface modification. The mole ratio of 0.5/1.0 between -OH and -COOH was an optimized one because in this case, higher degrees of crosslinking and better mechanical properties could be achieved [1].

[1] Qiu, Y. X.; Wanyan, Q. R.; Xie, W. Y.; Wang, Z. F.; Chen, M.; Wu, D. F. Green and biomass-derived materials with controllable shape memory transition temperatures based on cross-linked poly(*L*-malic acid). *Polymer* **2019**, *180*, 121733.

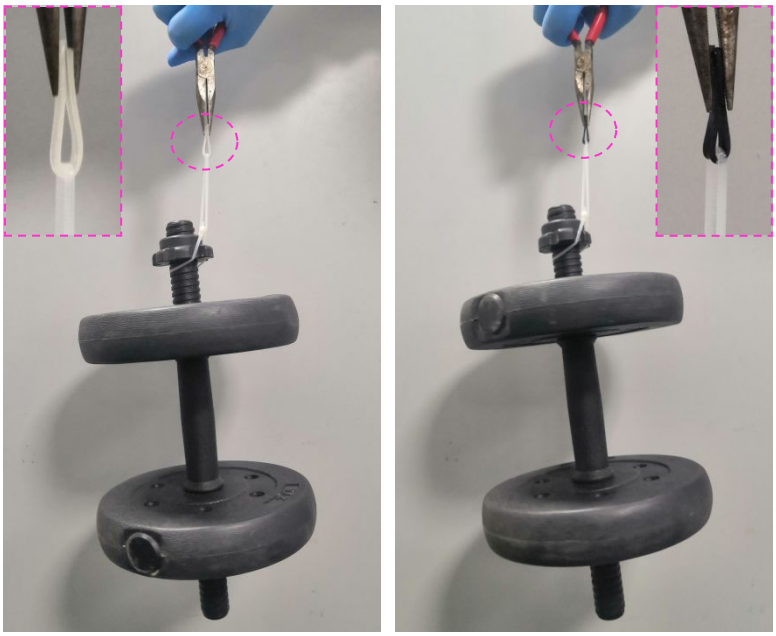

Figure S7. Pictures of cross-linked PLMA (left) and nanocomposites (0.2 wt% CNTs, right) samples loaded with 20 Kg dumbbell

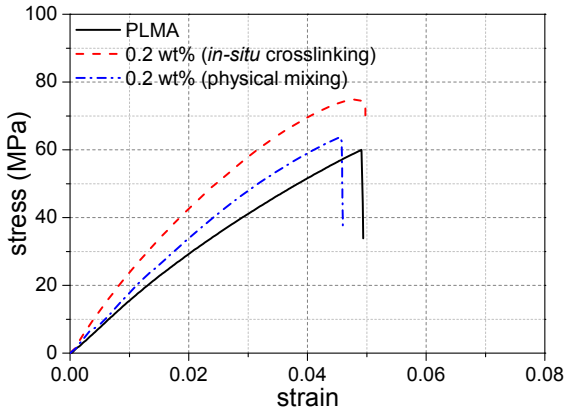

Figure S8. Stress-strain curves for the cross-linked PLMA and its nanocomposites (0.2 wt% CNTs) prepared by *in-situ* crosslinking and physical mixing

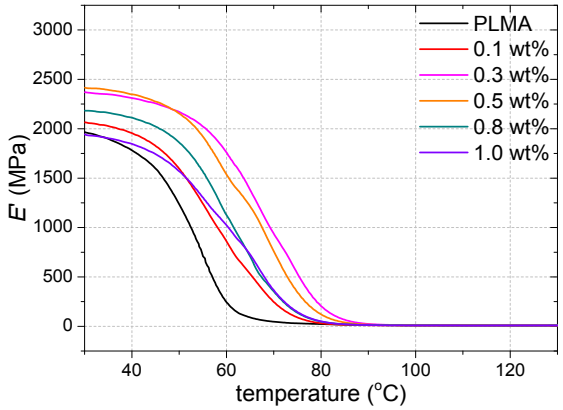

Figure S9. Storage moduli (*E*') of cross-linked PLMA and its nanocomposites with various CNT loadings

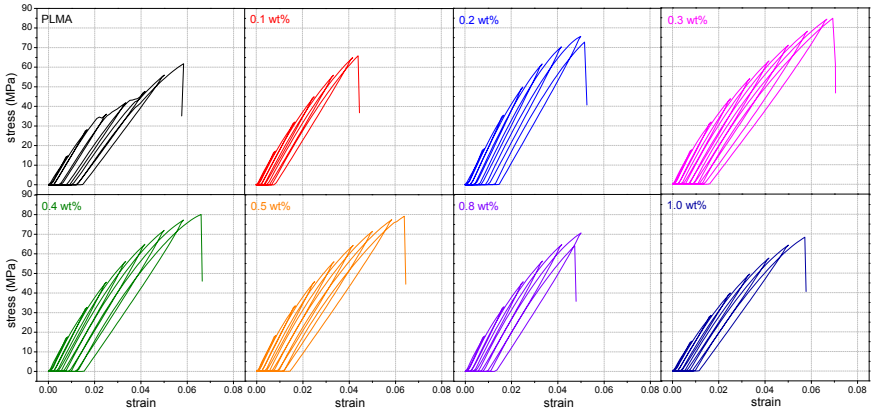

Figure S10. Cyclic stress-strain traces of cross-linked PLMA and its nanocomposites with various CNT loadings

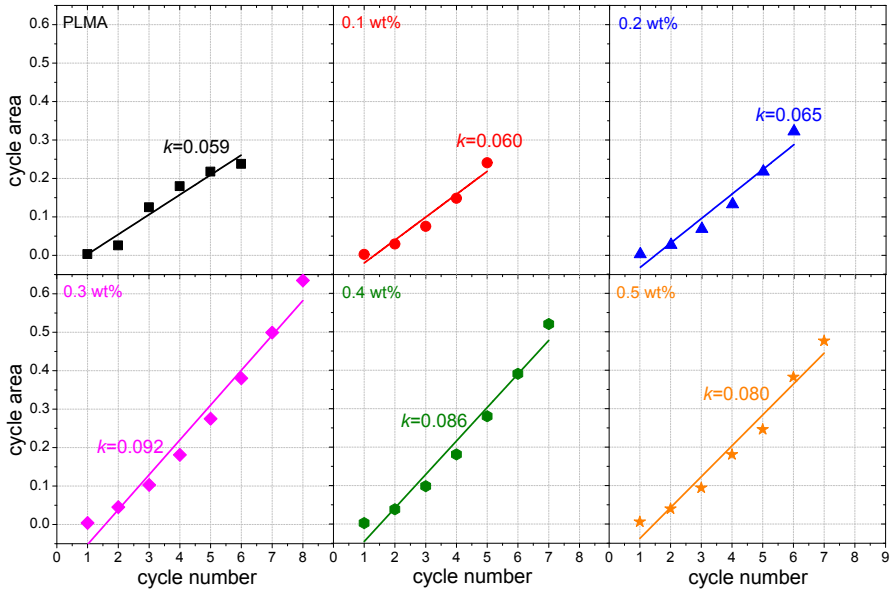

Figure S11. Hysteresis loop areas against tensile cycle numbers for cross-linked PLMA and its nanocomposites with various CNT loadings

Note: The hysteresis loop area is indicative of the work consumed in each cyclic test, which is a scale of mobility/relaxation level of chain segments. At the same stress levels in the same cyclic test (especially at the higher levels), the nanocomposite with 0.3 wt% CNTs shows the highest loop area, meaning that this sample has the strongest internal friction level among all samples. It is indicative of a balanced network structure in this sample, with optimized degree of crosslinking and better dispersion of CNTs, because relaxations of chain segments are restrained more strongly. This is to some degree in agreement with the highest T_g of this sample.

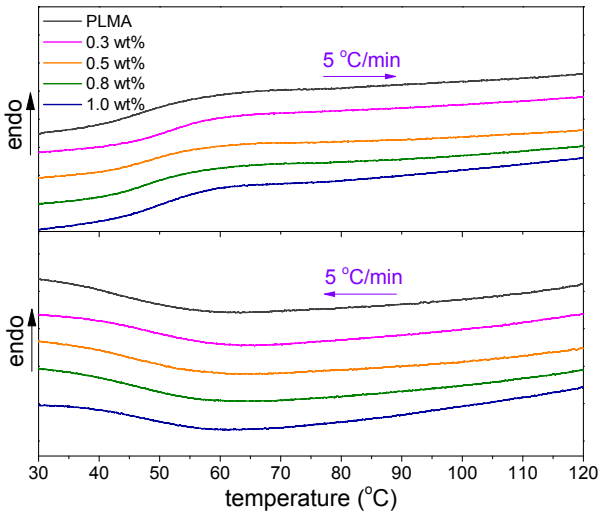

Figure S12. DSC traces of cross-linked PLMA and its nanocomposites with various CNT loadings

Note: No thermal events could be seen during heating/cooling scan, except thermal relaxations caused by glass transition.

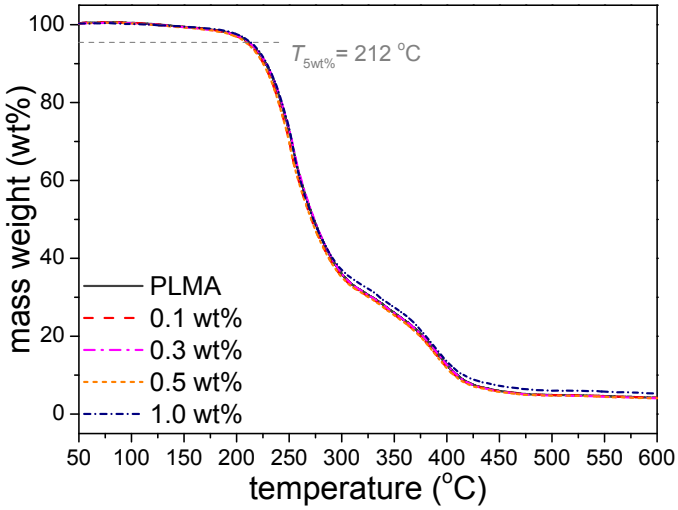

Figure S13. TGA curves for cross-linked PLMA and its nanocomposites with various CNT loadings

Note: Nanocomposites have almost the same 5 wt% mass loss temperature ($T_{5wt\%}$) with that of neat polymers. Therefore, the presence of CNTs within experimental loading range (0.1-1.0 wt%) does not affect thermal stability of cross-linked PLMA.

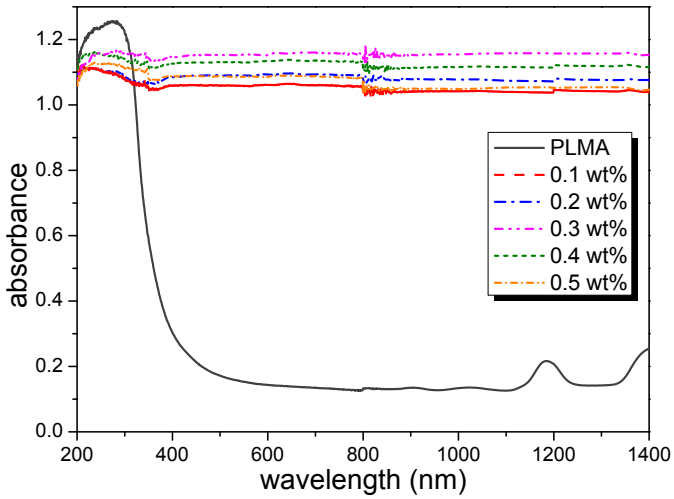

Figure S14. UV-vis-NIR absorbance curves for neat polymer and its nanocomposites with various CNT loadings

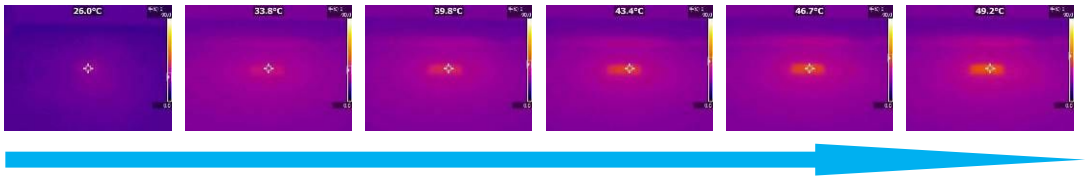

Figure S15. Infrared thermal images of the nanocomposite with 0.3 wt% CNTs under sunlight (100 mW cm^{-2}, taken every 20 s)

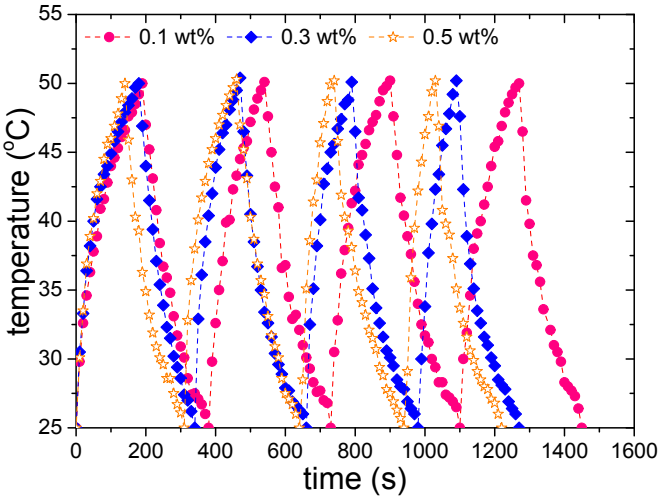

Figure S16. Surface temperature alterations with cyclic 'on & off' of sunlight (1000 mW cm^{-2}) for the nanocomposites with various loadings of CNTs

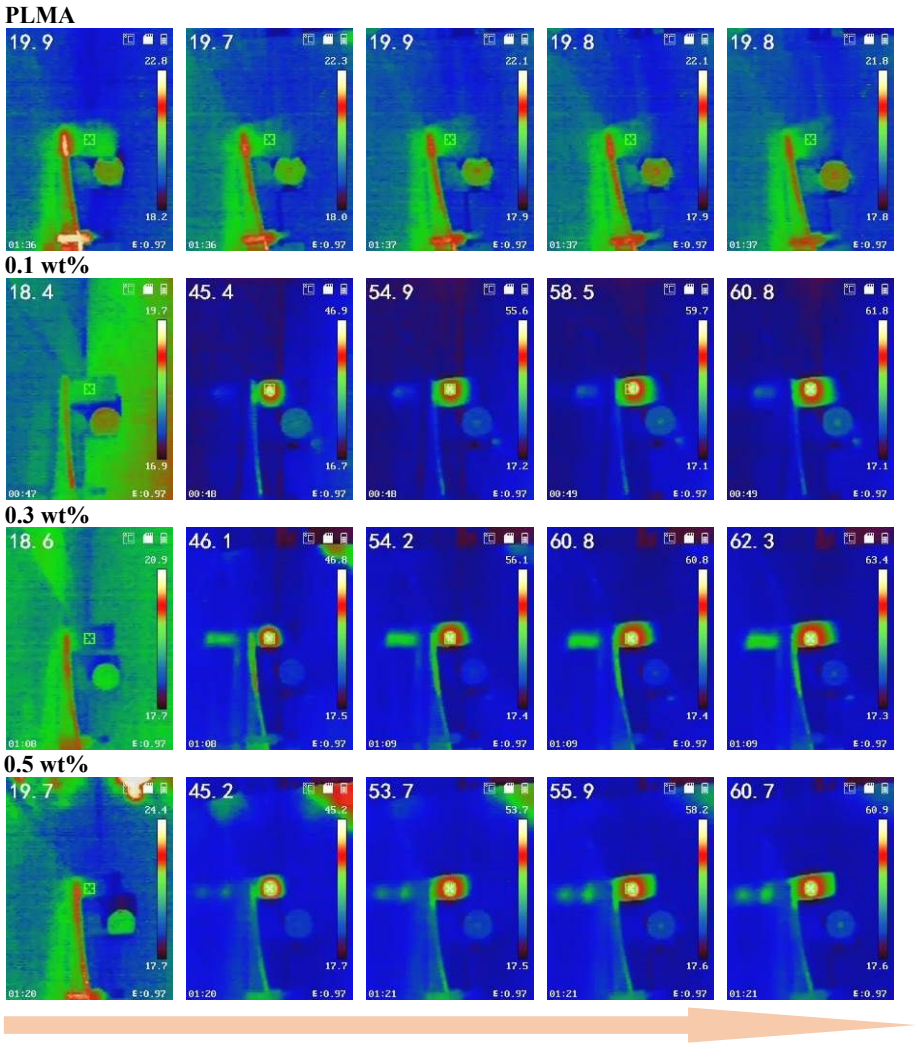

Figure S17. Infrared thermal images of neat polymer and the nanocomposites under 650 nm laser irradiation (50 mW cm^{-2}, taken every 20 s)

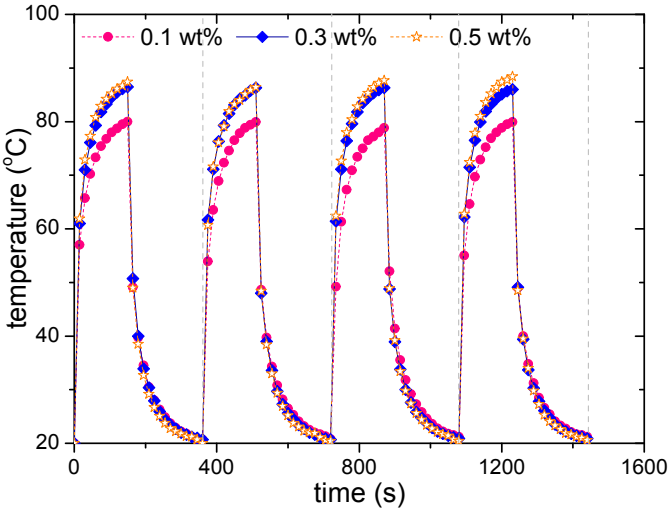

Figure S18. Surface temperature alterations with cyclic 'on & off' of laser irradiation (650 nm, 50 mW cm^{-2}) for the nanocomposites with various loadings of CNTs